Radiation Physics and Chemistry xxx (xxxx) xxx–xxx

Contents lists available at ScienceDirect

Radiation Physics and Chemistry

journal homepage: www.elsevier.com/locate/radphyschem

Estimate of S-values for children due to six positron emitting radionuclides used in PET examinations

Walmir Belinato[a], William S. Santos[b,c], Ana P. Perini[c], Lucio P. Neves[b,c], Linda V.E. Caldas[b], Divanizia N. Souza[d,*]

[a] Instituto Federal de Educação, Ciência e Tecnologia da Bahia (IFBA), Av. Amazonas, 3150, 45.100-000, BA, Brazil
[b] Instituto de Pesquisas Energéticas e Nucleares, Comissão Nacional de Energia Nuclear (IPEN-CNEN/SP); Av. Prof. Lineu Prestes, 2242, 05508-000 SP, Brazil
[c] Instituto de Física, Universidade Federal de Uberlândia (UFU), Av. João Naves de Ávila, 2121 Santa Mônica, 38400-902 Uberlândia, MG, Brazil
[d] Departamento de Física, Universidade Federal de Sergipe (UFS), Rod. Marechal Rondon, s/n, 49.100-000, SE, Brazil

ARTICLE INFO

Keywords:
Positron emission tomography
Monte Carlo
S-value

ABSTRACT

Positron emission tomography (PET) has revolutionized the diagnosis of cancer since its conception. When combined with computed tomography (CT), PET/CT performed in children produces highly accurate diagnoses from images of regions affected by malignant tumors. Considering the high risk to children when exposed to ionizing radiation, a dosimetric study for PET/CT procedures is necessary. Specific absorbed fractions (SAF) were determined for monoenergetic photons and positrons, as well as the S-values for six positron emitting radionuclides (^{11}C, ^{13}N, ^{18}F, ^{68}Ga, ^{82}Rb, ^{15}O), and 22 source organs. The study was performed for six pediatric anthropomorphic hybrid models, including the newborn and 1 year hermaphrodite, 5 and 10-year-old male and female, using the Monte Carlo N-Particle eXtended code (MCNPX, version 2.7.0). The results of the SAF in source organs and S-values for all organs showed to be inversely related to the age of the phantoms, which includes the variation of body weight. The results also showed that radionuclides with higher energy peak emission produces larger auto absorbed S-values due to local dose deposition by positron decay. The S-values for the source organs are considerably larger due to the interaction of tissue with non-penetrating particles (electrons and positrons) and present a linear relationship with the phantom body masses. The results of the S-values determined for positron-emitting radionuclides can be used to assess the radiation dose delivered to pediatric patients subjected to PET examination in clinical settings. The novelty of this work is associated with the determination of auto absorbed S-values, in six new pediatric virtual anthropomorphic phantoms, for six emitting positrons, commonly employed in PET exams.

1. Introduction

Positron emission tomography (PET) has been revolucionary in the diagnosis of cancer. When combined with computed tomography (CT), PET/CT performed in children produces a diagnosis of high accuracy on the images of regions affected by malignant tumors. Considering the high risk for children when exposed to ionizing radiation, a dosimetric study for PET/CT procedures is necessary (Xie et al., 2013).

The first dosimetry study using computational simulations utilized the MIRD Phantom (Medical Internal Radiation Dose), produced by Fisher and Snyder (1967). From this moment, with the development of tomography and computational techniques, the structure of the virtual anthropomorphic phantoms has been improved, allowing studies in patients with different structures (Zaid and Xu, 2007) and bodies with structural variations due to the breathing process (Xie and Zaid,).

Doses in the internal organs of patients are expressed as a function of the cumulative activity and of the S-values (mGy/MBq.s), as the MIRD method. The aim of this study is to determine the specific absorbed fractions (SAF) for monoenergetic photons and positrons, as well as the S-values for six positron emitting radionuclides, and 22 source organs. The study was conducted for six pediatric virtual anthropomorphic phantoms, including the newborn and 1 year hermaphrodite (Casssola et al., 2013), 5 and 10-year-old male and female (deMeloLima et al., 2011), using the Monte Carlo code (MCNPX) version 2.7.0 (Pelowitz, 2011). A study with pediatric anthropomorphic phantoms was also carried out in

* Corresponding author.
E-mail addresses: wbfisica@gmail.com (W. Belinato), william@ufu.br (W.S. Santos), anapaula.perini@ufu.br (A.P. Perini), lucio.neves@ufu.br (L.P. Neves), lcaldas@ipen.br (L.V.E. Caldas), divanizi@ufs.br (D.N. Souza).

http://dx.doi.org/10.1016/j.radphyschem.2017.02.038
Received 30 September 2016; Received in revised form 13 February 2017; Accepted 17 February 2017

Table 1
Main characteristics of the pediatric virtual anthropomorphic phantoms utilized in this work.

Pediatric phantom	Mass (kg)	Height (cm)	Matrix[a]	BMI (kg/m^2)
Newborn (NB)	3.55	50.50	135×99×361	14.00
1 Year-old (1-Y)	10.25	76.00	190×135×543	17.70
5 Years-old-male (M5)	19.46	109.13	284×143×780	16.34
5 Years-old-female (F5)	19.43	109.13	284×143×780	16.32
10 Years-old-male (M10)	32.86	138.11	353×157×987	17.22
10 Years-old-female (F10)	32.80	138.11	353×157×987	17.20

[a] column×line×slice.

the work of Xie et al. (2013), for several positron-emitting radionuclides, but employing anthropomorphic pediatric hybrid models, which are different of those employed in this work. The irradiation scenarios considered patients lying on a bed inside a PET/CT room.

2. Materials and methods

2.1. Virtual anthropomorphic phantoms

In this work, we utilized a pediatric phantom series, including the reference newborn, 1, 5, and 10-year-old male and female models, for radiation dosimetry calculations. They were built utilizing MESH (set of vertices, edges and faces that define the object shape in 3D computer graphic) (Casssola et al., 2013; deMeloLima et al., 2011). These phantoms were developed by the Radiation Dosimetry Group/Federal University of Pernambuco, Brazil, and they have more than 100 organs and segmented tissues, which make them very useful for computational dosimetry. Some important characteristics of the pediatric virtual anthropomorphic phantoms used in this work, such as weight, height, dimensions of the matrix and body mass index (BMI), are presented in Table 1.

The MIRD method (Medical Internal Radiation Dose), Pamphlet No. 21 (Bolch et al., 2009) shows the absorbed dose rate at a target organ (r_T) due to a source organ (r_S) from Eq. (1):

$$\dot{D}(r_T, t) = \sum_{r_S} \widetilde{A}_{(r_S,t)} S_{(r_T \leftarrow r_S,t)} \quad (1)$$

where $\widetilde{A}_{(r_S,t)}$ is the cumulative radionuclide activity in the source organ and $S_{(r_T \leftarrow r_S,t)}$ is the S-value expressed in terms of the fraction of the energy emitted by the source-organ deposited in the target organ.

The results of the doses to the internal organs of patients are expressed as a function of administered activity. Careful choices of source organ inside of the virtual anthropomorphic phantoms are needed to determine these doses, as well as a detailed description of the sources in the computational scenarios (Stabin, 2008).

To determine the S-values and the specific absorbed fractions (SAF) for positron emitting radionuclides in target organs, we used Eqs. (2) and (3), respectively (Bolch et al., 2009):

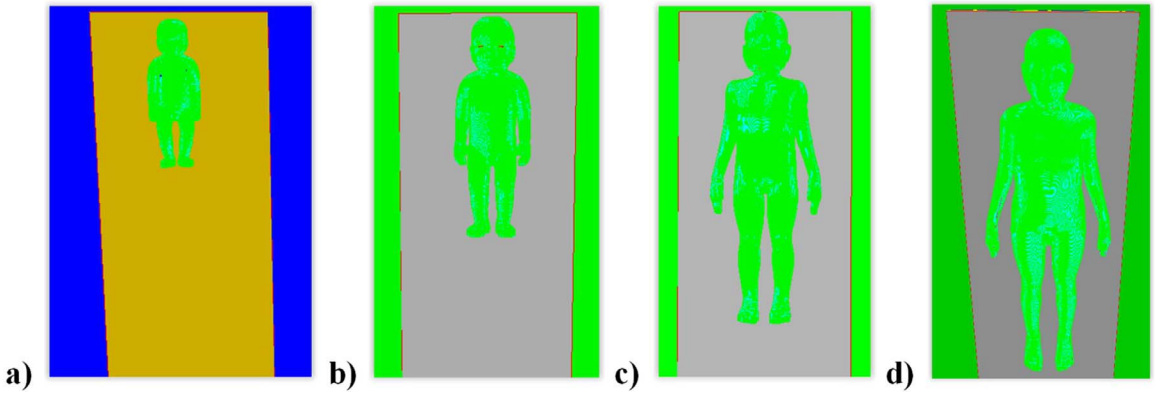

Fig. 1. Irradiation MCNPX PET scenarios: (a) Newborn (NB) (b) 1 year-old (1Y) (c) 5 years-old male (M5) d) 10 years old male (M10).

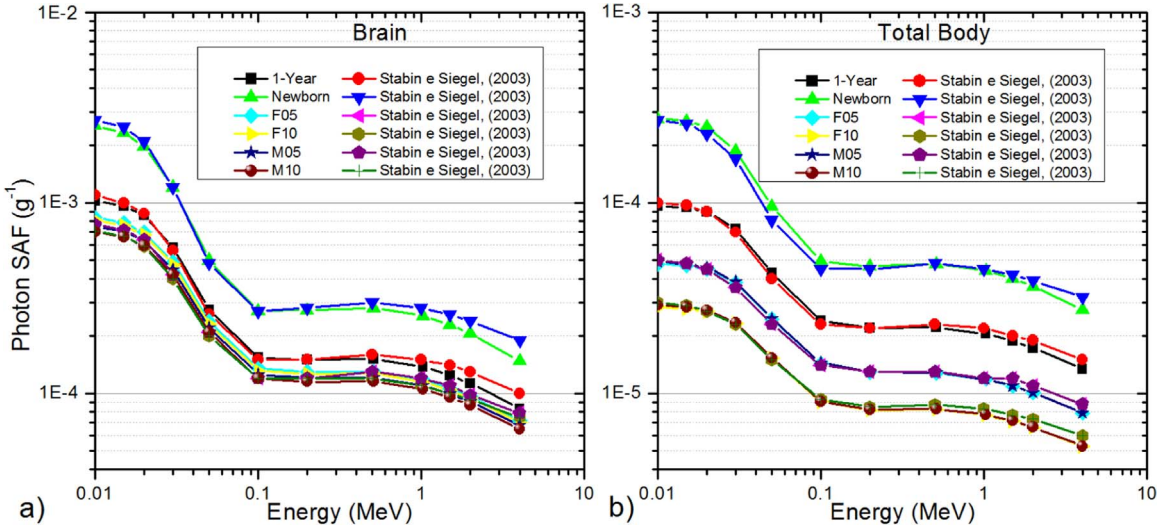

Fig. 2. SAF for the pediatric virtual anthropomorphic phantoms (a) Brain (b) Total Body.

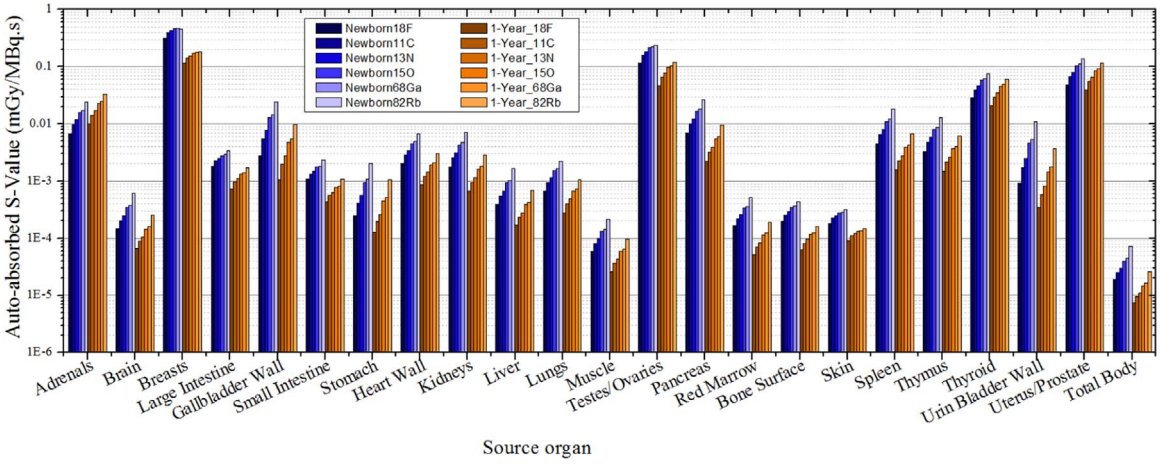

Fig. 3. Auto absorbed S-values in the newborn and 1-year-old pediatric virtual anthropomorphic phantoms.

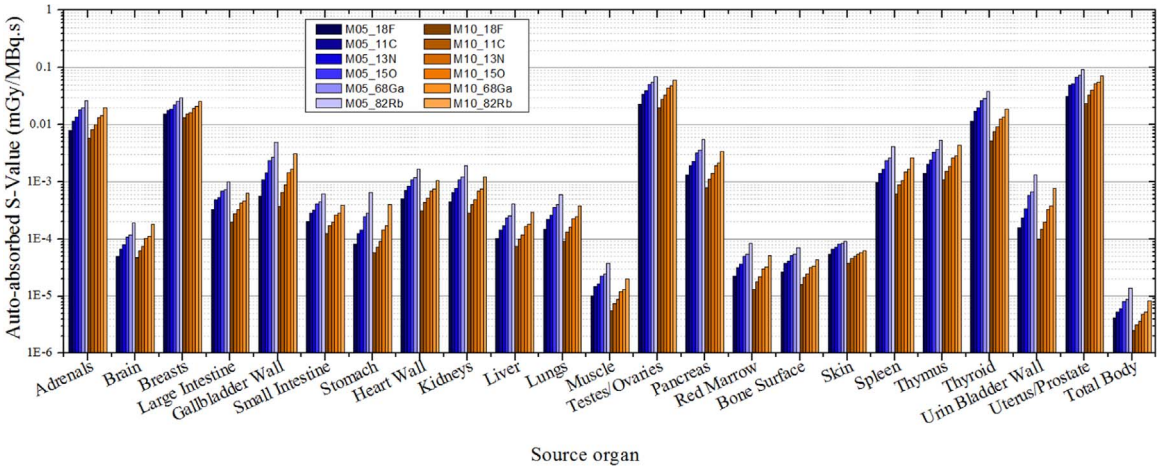

Fig. 4. Auto absorbed S-values in M05 and M10 male virtual anthropomorphic phantoms.

$$S_{(r_T \leftarrow r_S, t)} = \sum_i \frac{\Delta_i \phi(r_T \leftarrow r_S, E_i, t)}{M_{(r_T, t)}} \quad (2)$$

$$\phi_{(r_T \leftarrow r_S, E_i)} = \frac{E_{(S)}}{E_{(T)}} \quad (3)$$

In the Eq. (2), Δ_i and $\phi(r_T \leftarrow r_S, E_i, t)$ are the emission energies and fractions of absorbed energies by the target organs, respectively. $M_{(r_T,t)}$ is the mass of the target organ. The fractions of absorbed energies described by Eq. (3) depend on the energy emitted by the target organ ($E_{(T)}$) and on the energy emitted by the source organ ($E_{(S)}$).

Fig. 1 shows the PET irradiation scenarios, with images of pediatric anthropomorphic phantoms used in this study. The phantoms were positioned lying on a bed, composed of three layers: carbon fiber + polyethylene, polyethylene and metallic alloy.

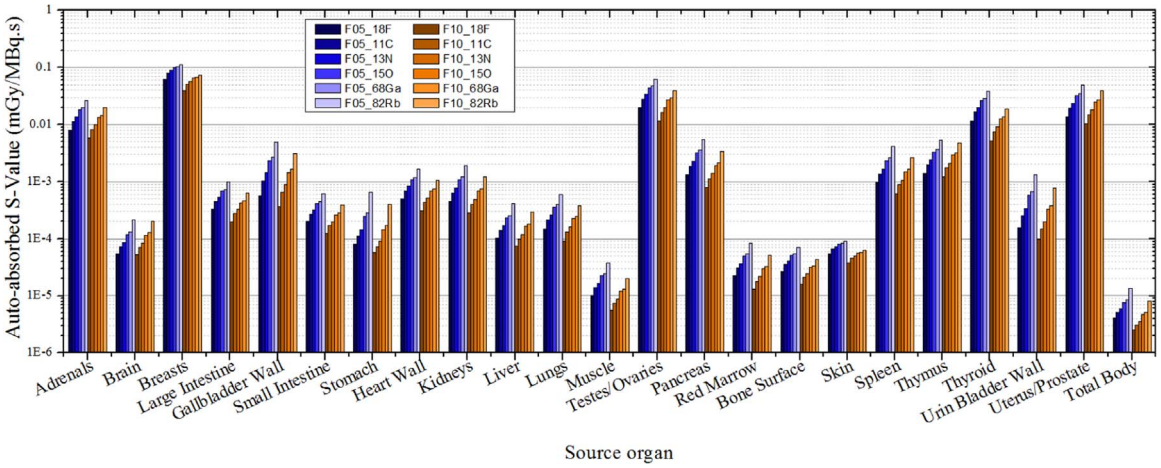

Fig. 5. Auto absorbed S-values in the F05 and F10 female virtual anthropomorphic phantoms.

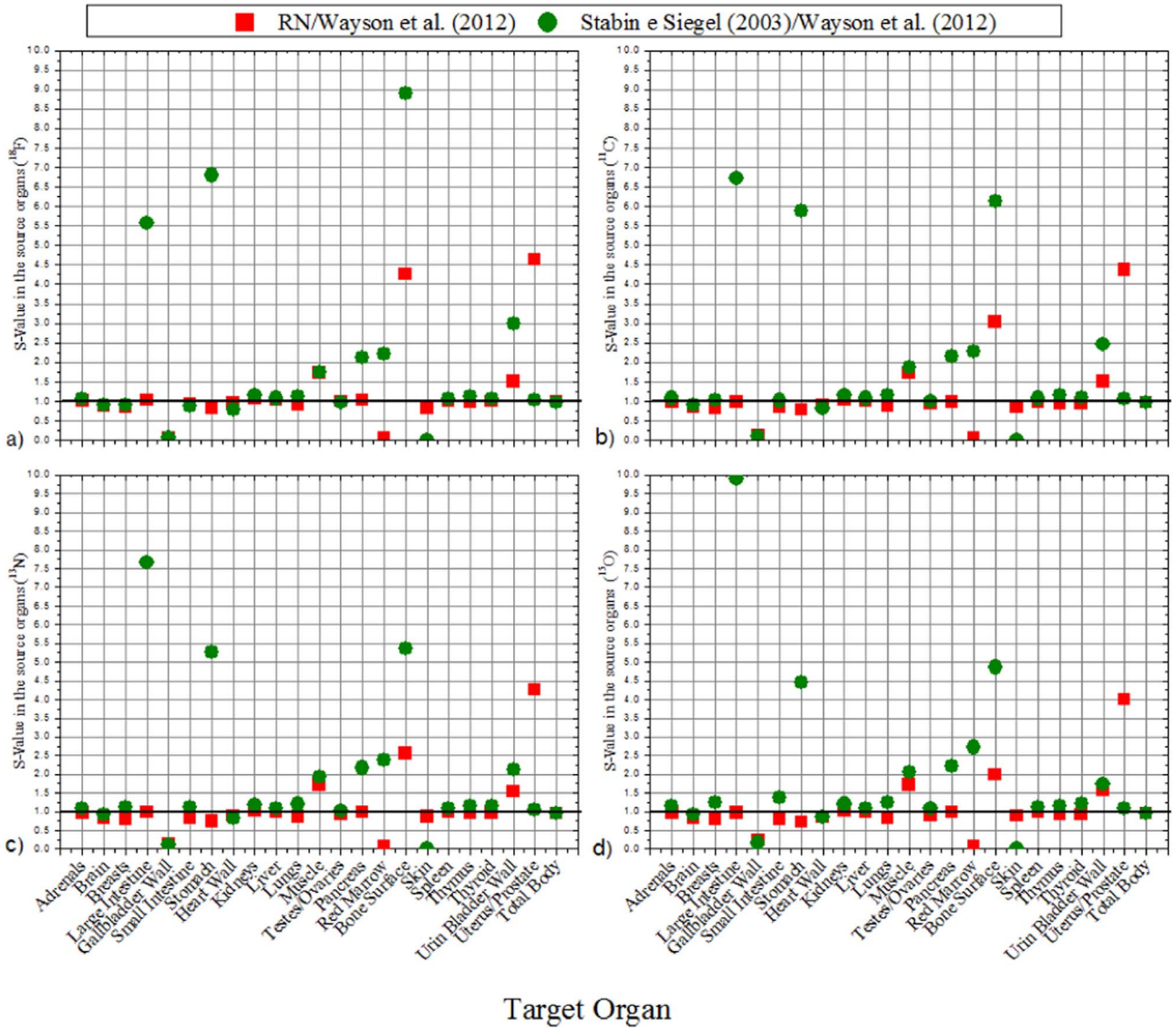

Fig. 6. S-values absorbed in the source organs for newborn phantom (RN) obtained in this study and the results of Wayson et al. (2012) and of Stabin and Siegel (2003) for (a) ^{18}F (b) ^{11}C c) ^{13}N e (d) ^{15}O.

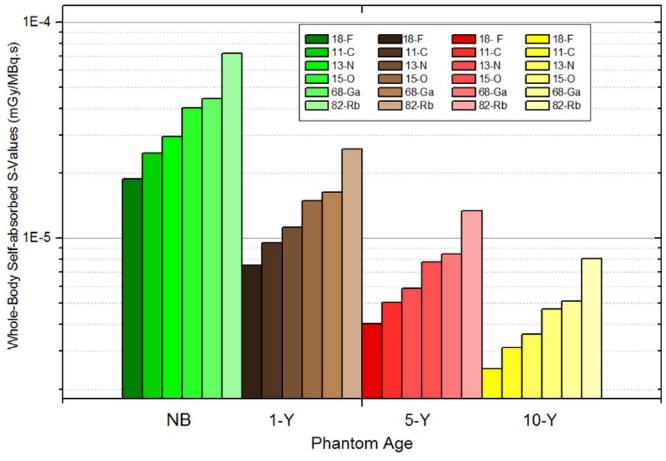

Fig. 7. Relationship between auto absorbed S-value, phantom age and radionuclides.

2.2. Monte Carlo simulations conditions

The Monte Carlo code used in this study was the Monte Carlo N- Particle – eXtended MCNPX (Pelowitz, 2011).

In the simulations, we considered the transport of photons and electrons, due to positron annihilation in the source organs. The positron emission spectra were available from the RADAR system for the following radionuclides: ^{18}F, ^{11}C, ^{13}N, ^{15}O, ^{68}Ga, and ^{84}Rb (Eckerman and Endo, 2008).

In this study we used Eq. (4) to determine the S-value in the organs of interest, given in units of mGy/MBq.s:

$$S_{(r_T \leftarrow r_S,t)} = \frac{Tally\ ^*F8}{M_{r_T}}(1.602E-04) \quad (4)$$

where $Tally\ ^*F8$ is a MCNP card, that may provide the energy distribution in a cell. It is analogous to a radiation detector. Each history will deposit its energy, and it will be separated in channels. Its units are given in units of energy (MeV). This energy was deposited in the target organs, where M_{r_T} is the mass of the target organ [kg] and 1.602E-04 is the conversion constant from MeV to Joule (J),

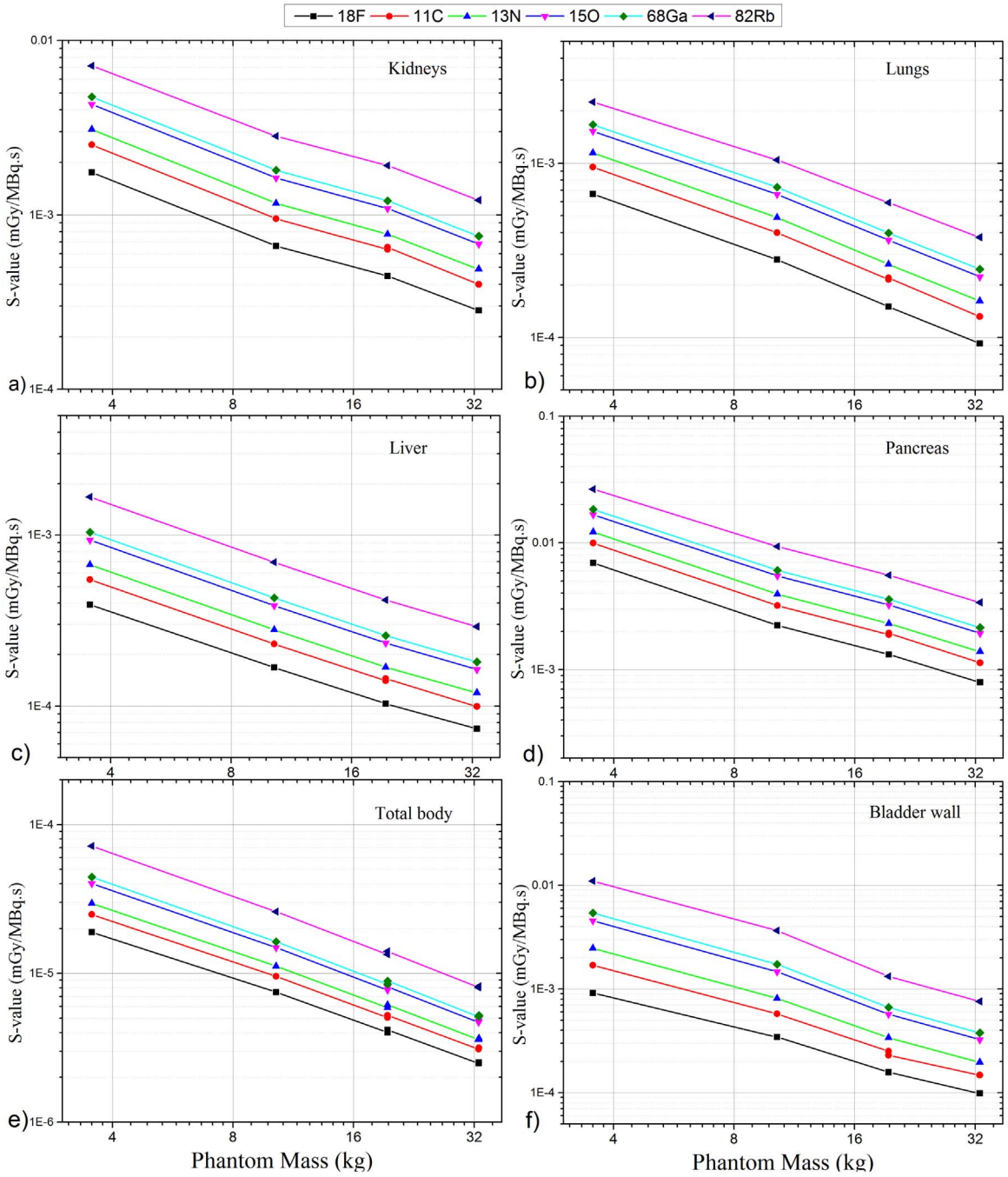

Fig. 8. S-values in source organs as a function of the body mass (kg) for: (a) kidneys, (b) lungs, (c) liver, (d) pancreas, (e) total body and (f) bladder wall.

considering the unity to the activity (MBq) and the unity to absorbed dose (mGy). The doses for PET/CT vary with the administered radionuclide activity and the parameters used in the CT scan. In this case, the administered activity is in MBq range and absorbed dose in mGy.

The results of auto-absorbed S-values obtained in this work were compared to literature results (Stabin and Siegel, 2003;Wayson et al., 2012), for the same positron emitting radionuclides.

In the simulations the positron emitter was homogenously distributed in the source organs. For all computational calculations, 10^7 initial particles were simulated. This parameter provided statistical uncertainties below 5% for the S-values in the internal organs of the virtual anthropomorphic phantoms.

3. Results and discussion

The results of SAF are shown in Fig. 2. Here, we present only the results of the brain and the whole body as regions of high absorption of radiopharmaceuticals. The other organs showed variations in the curves of the SAF similar to variations to the brain and the total body.

It may be observed that the results of specific fractions of photons absorbed in the brain, Fig. 2(a), and total body, Fig. 2(b), are analogous to those presented by Stabin and Siegel (2003), since the masses of these regions are similar, and the differences in their shapes do not significantly affect these results. It can also be noted that moderate and

high photon energy above 0.511 MeV in the pediatric phantom, cross the structure bodies depositing less energy. For doses due to positron emitters, photons with well-defined energy (0.511 MeV) are produced, and the variations observed in SAF can be neglected. For energies below 0.511 MeV we found differences up to 50% when compared to the literature (Stabin and Siegel, 2003).

The SAF values present small increases, in relation to those of Stabin and Siegel (2003), due to the geometrical proximity of the organs, more realistic than those from mathematical phantoms (employed in the work of Stabin and Siegel (2003)). The mathematical phantoms present organs with a higher separation (which is also less realistic). Simular variations where found by Stabin et al. (2012); Xie et al. (2013), for the SAF, when comparing mathematical phantoms and NURBS-based phantoms.

The results of auto absorbed S-values are shown in Figs. 3, 4 and 5 for newborn, 1-year, 5-years and 10-years old virtual anthropomorphic phantoms, respectively.

The results obtained in this study are in agreement with the values obtained by Wayson et al. (2012), as shown in Fig. 6.

The ^{82}Rb produces the highest S-values for source organs due to its higher energy positron emission.

The obtained S-values showed to be dependent on the resolution and size of the voxel corresponding to (6.63×6.63×6.63) cm^3 utilized by Wayson et al. (2012) and (1.4×1.4×1.4) cm^3 utilized in this study.

Similar conclusions were observed in literature (Xie et al., 2013), using a virtual anthropomorphic phantom with voxel resolution of (1.8×1.8×3.0) cm^3. The ratios of the S-values found in the literature (Stabin and Siegel, 2003; Wayson et al., 2012) vary between 0.21 and 2.32. These differences could be attributed to the differences between the model geometry using mathematical equations, and based voxel structures (Wayson et al., 2012). Similar results were obtained in other publications (Xie et al., 2013; Belinato et al., 2014).

In the MIRD Pamphlet No. 11 (Snyder et al., 1975) the S-values of photons with energies above 0.100 MeV in source organs are proportional to the mass of the organs raised to the power of two-thirds ($m^{2/3}$). In the UF-NCI hybrid phantoms, to radionuclides (^{11}C, ^{18}F, ^{68}Ga, ^{82}Rb, ^{13}N), more than 70% of the S-values are the result of the positron interactions (Xie et al., 2013). To organs far from the source, considering ^{11}C, ^{18}F or ^{68}Ga, more than 80% in of the S-value results are due to photon annihilation (0.511 MeV). Therefore, increasing the BMI of the virtual anthropomorphic phantoms, the contribution of photons to the S-values becomes higher, and that of positrons becomes lower (Xie et al., 2013; Wayson et al., 2012; Belinato et al., 2014). This aspect needs to be discussed more carefully in order to estimate the contribution of each type of radiation in the S-value results, especially in pediatric virtual anthropomorphic phantoms.

Fig. 7 shows the auto absorbed S-values in total-body for each pediatric phantom and radionuclide. The S-values present higher values, for radionuclides with higher energy emissions for all phantoms studied. For ^{18}F and ^{82}Rb, for example, the average energies of positrons are 0.206 MeV and 1.09 MeV, respectively.

For all radionuclides, the S-values, at the source organs, decrease with the increase of the body mass, as presented in Fig. 8, for some source organs.

4. Conclusions

The results of the SAF in source organs, and S-values for all organs, were inversely related to the age of the phantoms, which includes the variation of body weight. The results also showed that radionuclides, with higher energy peak emission, produce higher auto absorbed S-values due to local deposition of energy by positron decay. The S-values for the source organs are considerably larger due to the interaction of tissue with non-penetrating particles (electrons and positrons) and have a linear relationship with the masses of the bodies. The results of the S-values determined for positron-emitting radionuclides can be used to assess the radiation dose delivered to pediatric patients subjected to PET examination in clinical settings.

Acknowledgements

The authors would like to thank the Brazilian agencies: CAPES (Project Pró-Estratégia 1999/2012), CNPq (Grants No. 304789/2011-9, 501857/2014-1 and 157593/2015-0), MCT: Project INCT for Radiation Metrology in Medicine, and Fundação de Amparo à Pesquisa do Estado de Minas Gerais (FAPEMIG, Project No. APQ-03049-15 and APQ-02934-15).

Appendix A. Supplementary data

Supplementary data associated with this article can be found in the online version at http://dx.doi.org/10.1016/j.radphyschem.2017.02.038.

References

Belinato, W., Santos, W.S., Silva, R.M.V., Souza, D.N., 2014. Monte Carlo estimation of radiation dose in organs of female and male adult phantoms due to FDG-F18 absorbed in the lungs. EPJ Web Conf. 66 (100002), 1–4.

Bolch, W.E., Eckerman, K.F., Sgouros, G., Thomas, S.R., 2009. MIRD Pamphlet No. 21: a generalized schema for radiopharmaceutical dosimetrystandardization of nomenclature. J. Nucl. Med. 50 (3), 477–484.

Casssola, V.F., Kramer, R., Melo Lima, V.J., Lira, C.A.B.O., Khoury, H.J., Vieira, J.W., Bronw, K.R., 2013. Development of newborn and 1-year-old reference phantoms based on polygon mesh surfaces. J. Radiol. Prot. 33, 669–691.

de Melo Lima, V.J., Cassola, V.F., Kramer, R., Lira, C.A.B.O., Khoury, H.J., Vieira, J.W., 2011. Development of 5 and 10 years old infant phantoms based on polygonal meshes. Med. Phys. 38 (8), 4723–4736.

Eckerman, K.F., Endo, A., 2008. Radionuclide Data and Decay Schemes 2nd edition. Society for Nuclear Medicine, Reston, VA.

Fisher, H.L., Snyder, W.S., 1967. Report. Oak Ridge National Laboratory ORNL-4168.

Pelowitz, D.B., 2011. MCNPX User's Manual, Version 2.7.0, Los Alamos National Laboratory report LA-CP-11–00438.

Snyder, W.S., Ford, M.R., Warner, G.G., Watson, S.B., 1975. MIRD Pamphlet No: S Absorbed Dose Per Unit Cumulated Activity for Selected Radionuclides and Organs. The Society of Nuclear Medicine, New York, 11.

Stabin, M.G., 2008. Fundamentals of Nuclear Medicine Dosimetry. Springer, (ISBN: 978-0-387-74578-7).

Stabin, M.G., Siegel, J.A., 2003. Physical models and dose factors for use in internal dose assessment. Health Phys. 85 (3), 294–310.

Stabin, M.G., Emmons, M.A., Segars, W.P., Fernald, M.J., 2012. Realistic reference adult and paediatric phantom series for internal and external dosimetry. Radiat. Prot. Dosim. 149 (1), 56–59.

Wayson, M., Lee, C., Sgouros, G., Treves, S.T., Frey, E., Bolch, W.E., 2012. Internal photon and electron dosimetry of the newborn patient-a hybrid computational phantom study. Phys. Med. Biol. 57, 1433–1457.

Xie, T., Zaid, H., Effect of respiratory motion on internal radiation dosimetry. Med. Phys. 41 (11): 112506.

Xie, T., Bolch, W.E., Lee, C., Zaidi, H., 2013. Pediatric radiation dosimetry for positron-emitting radionuclides using anthropomorphic phantoms. Med. Phys. 40 (10), 1–14.

Zaid, H., Xu, X.G., 2007. Computational anthropomorphic models of the human anatomy: the path to realistic monte carlo modeling in radiological sciences. Annu. Rev. Biomed. Eng. 9, 471–500.